

Microstructure refinement by a novel friction-based processing on Mg-Zn-Ca alloy

CHEN Ting^{1,a*}, FU Banglong^{1,b}, SHEN Junjun^{1,c}, SUHUDDIN Uceu F.H.R.^{1,d},
WIESE Björn^{2,e}, DOS SANTOS Jorge F.^{3,f}, BERGMANN Jean Pierre^{4,g} and
KLUSEMANN Benjamin^{1,5,h}

¹Solid State Materials Processing, Institute of Material Mechanics, Helmholtz-Zentrum Hereon, Max-Planck-Str. 1, 21502 Geesthacht, Germany

²Functional Magnesium Materials, Institute of Metallic Biomaterials, Helmholtz-Zentrum Hereon, Max-Planck-Str. 1, 21502 Geesthacht, Germany

³Applied Materials and Manufacturing, Energy and Environment Division, Pacific Northwest National Laboratory, PO Box 999, Richland, 99352 WA, USA

⁴Production Technology Group, Technische Universität Ilmenau, Gustav-Kirchhoff-Platz 2, 98693 Ilmenau, Germany

⁵Institute for Production Technology and Systems, Leuphana University of Lüneburg, Universitätsallee 1, 21335 Lüneburg, Germany

^ating.chen@hereon.de, ^bbanglong.fu@hereon.de, ^cjunjun.shen@hereon.de,
^duceu.suhuddin@hereon.de, ^ebjoern.wiese@hereon.de, ^fjorge.dos.santos@hereon.de,
^gjeanpierre.bergmann@tu-ilmenau.de, ^hbenjamin.klusemann@hereon.de

Keywords: Constrained Friction Processing, Magnesium Alloys, Microstructure

Abstract. Insufficient mechanical properties and uncontrollable degradation rates limit the wide application of Mg alloys in bioimplant materials. Microstructure refinement is a common method to improve both the mechanical properties and the corrosion resistance of Mg alloys. In order to efficiently obtain Mg alloys with fine microstructures for potential applications in bioimplant materials, a novel constrained friction processing (CFP) was proposed. In this work, the resulting compression properties of ZX10 alloy obtained by CFP with optimized processing parameter are reported. Additionally, the microstructure evolution during CFP was studied. The results show that during CFP, materials are subjected to high shear strain at the transition zone between the stir zone and thermo-mechanical affected zone, leading to recrystallization with strong local basal fiber shear texture. As the shoulder plunges down, the fraction of recrystallized grain and grain size increase. ZX10 alloy obtained by CFP exhibited higher compressive yield strength by more than 300% and ultimate compressive strength improves by 60%, which indicates the bright prospect of CFP for Mg processing.

Introduction

Magnesium (Mg) alloys represent a prominent choice for biodegradable implants owing to their notable biocompatibility and biodegradability characteristics. The density and elastic modulus of Mg alloys closely resemble those of natural bones, thereby mitigating mechanical mismatches between the implant and bone in comparison to alternative alloys. Moreover, magnesium constitutes an essential element in the human body, and its alloys possess inherent biodegradability, obviating the necessity for subsequent surgical interventions. Within medical contexts, Mg alloys predominantly find utility as scaffolds for tissue engineering, implants for bone repair, and stents for cardiovascular applications.

However, Mg alloys with innocuous chemical compositions typically exhibit inadequate strength and corrosion resistance, which limits their use as biodegradable implants [1]. One

solution is to modify the microstructure of the alloys. Modifying the microstructure to achieve a finer grain size and secondary phases is beneficial for improving both mechanical properties and biocorrosion resistance [2]. Thermo-mechanical processing (TMP) methods, such as hot rolling [3] and hot extrusion [4], have been adapted to refine grains and secondary phases of as-cast Mg alloys. Additionally, severe plastic deformation (SPD) processing, such as equal-channel angular pressing (ECAP) [5] and high-pressure torsion (HPT) [6], have been developed to achieve a much finer microstructure.

While TMP and SPD have been shown to refine the microstructure and have potential for use in processing biodegradable Mg alloys with sufficient mechanical properties and corrosion resistance, there are still limitations. The microstructure resulting from a single TMP or SPD method is typically inhomogeneous, exhibiting shear zones [7], large deformed grains [8], and concentration of secondary phases [9]. This is due to insufficient or inhomogeneous deformation, which can result in weak mechanical strength and inhomogeneous corrosion properties. Therefore, these methods usually require multiple passes [10] or cooperation with long-time pre-heat treatment to achieve a homogeneous microstructure [11]. Additionally, samples obtained with certain SPD methods, such as HPT, may have limited dimensions.

The present work employs a new friction-based processing method, called constrained friction processing (CFP) [12,13]. This method has several advantages over other methods mentioned above. Firstly, it does not require external heating as the heat is generated by the friction between the tool and materials as well as plastic deformation. Secondly, it subjects materials to high strain and strain rates, and the optimized processing time is much shorter (approximately 3 seconds). Materials are stirred thoroughly and homogeneously, so additional pre-heating is unnecessary to homogenize the microstructure beforehand. The primary objective of this study is to fabricate defect-free, fine-grained Mg alloys with superior mechanical properties from a large-grained state of as-cast ZX10 using CFP for potential applications as bioimplant materials. The overall microstructure evolution was analyzed using the “stop-action” technique.

Materials and Method

The materials used in this work were conventional chill-casting Mg-1Zn-0.3Ca (wt.%) alloy (ZX10), with higher Zn content than ZX00, which has been reported in [13]. The average grain size of as-cast ZX10 alloys is more than 1 mm, see Fig. 1(a). The ZX10 ingot was cut into specimens with a dimension of $100 \times 25 \times 6 \text{ mm}^3$, and then cleaned by alcohol prior to processing.

The novel CFP is shown in Fig. 1. A tool system consists of a clamping ring, a shoulder and a probe. First of all, the specimen is compressed by the clamping ring to the backing. Then the shoulder rotates and plunges down into the material, and at the same time, the probe rotates and retracts. The friction between the rotating tool and material generates heat to plasticize the material. Finally, when the shoulder reaches the set depth, the tool system stops rotating and is removed from the material. After processing, a rod with the same diameter as the probe is obtained.

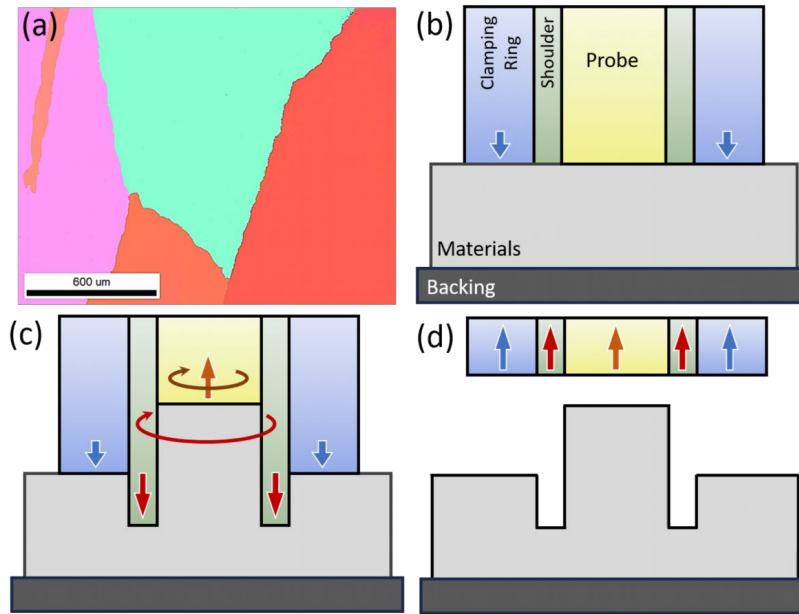


Fig. 1 (a) Microstructure and (b-d) Schematic drawing of procedure of CFP

In this work, the processing was performed on the refill FSSW machine RPS200 produced by Harms & Wende. The diameter of the clamping ring, shoulder and probe were 17 mm, 9 mm and 6 mm, respectively. The processing force was set as 12 kN. The maximum plunge depth of the shoulder was set as 3 mm, and the total plunge time was 3 s, resulting in an average plunge speed of 1 mm/s. To keep the volume of materials balanced, the retraction speed of the probe was set as 1.25 times plunge speed of the shoulder. The rotation speed of the shoulder and probe was the same, keeping 1800 rpm during processing.

Specimens were machined to a cylindrical sample with a diameter of 6 mm and a height of 6 mm for compression tests. These were carried out at room temperature using a Zwick/Roell 1478 universal testing machine at a strain rate of 10^{-3} s^{-1} . Compressive yield strength, ultimate compressive strength and elongation were evaluated by the average of three specimens per processing parameter.

In order to characterize the microstructure of the rod obtained by CFP, the longitudinal-section of the rod was ground and polished according to standard metallographic sample preparation. Then, the sample was electricity polished using AC2 solution using voltage 25 V at $-20 \text{ }^\circ\text{C}$ for 35 s. An FEI Quanta 650 field emission gun (FEG) SEM equipped with electron backscattered diffraction (EBSD) detectors was used to further analyze the microstructure. The data from EBSD were analyzed by TSL OIM 7.3, respectively. The volume fraction of recrystallized grain was calculated according to Grain Orientation Spread (GOS) obtained by EBSD. The grains with GOS lower than 2° are defined as recrystallized grains, while those with GOS higher than 2° are deformed grains.

Results

Microstructure

Fig. 2 displays the microstructure of various subregions in the ZX10 rod obtained through CFP with moderate heat input at a rotation speed of 1800 rpm and a plunge speed of 1 mm/s. The average grain size after CFP decreased significantly compared to the as-casted ZX10 alloy, being the primary reason for the improvement in compression strength. The rod's average grain size is

approximately 5-6 μm , as shown in the IPF images in Fig. 2. The grain size in the horizontal direction is similar from the axis center to the edge.

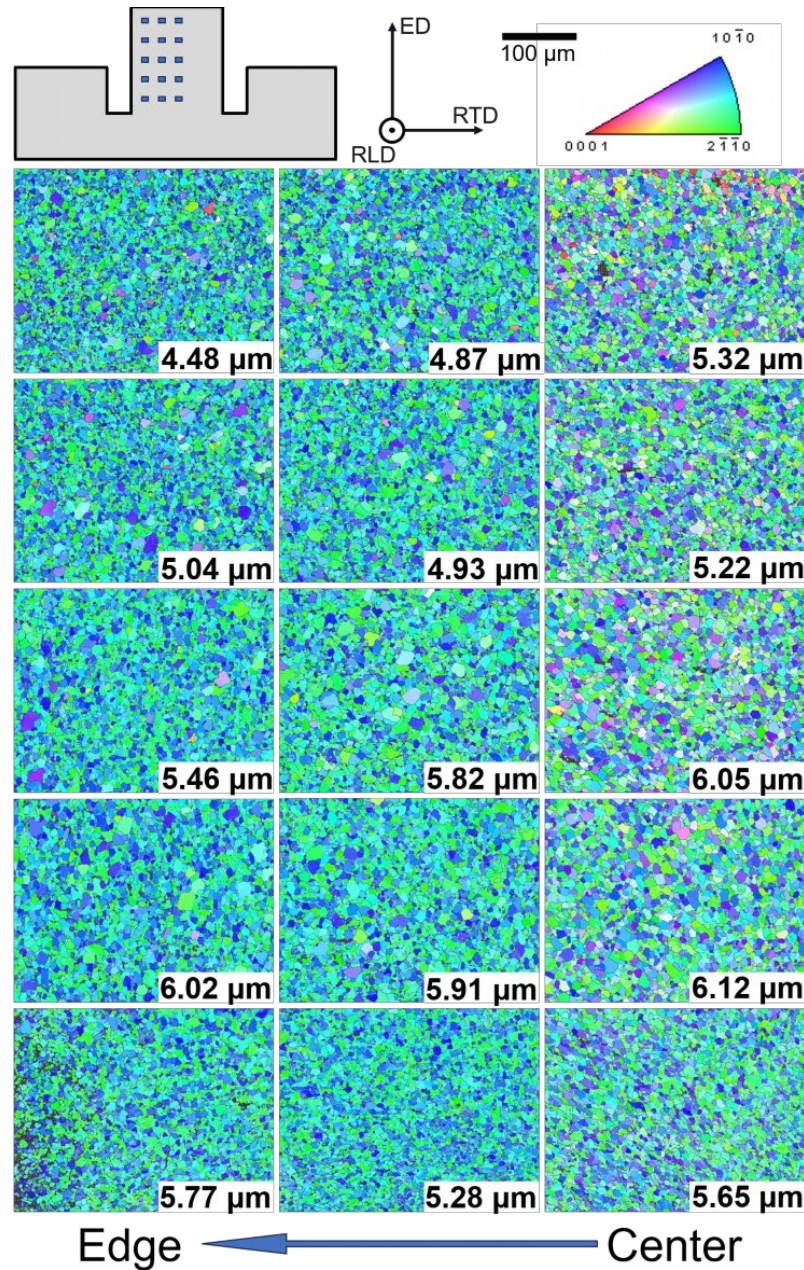


Fig. 2 Inverse pole figures (IPF) of ZX10 obtained by CFP with rotation speed of 1800 rpm and plunge speed of 1 mm/s corresponding to the position marked by blue rectangle. The average grain size is labeled at the lower right corner.

The [0002] pole figures (PFs) in Fig. 3 show the analyzed textures of the observed subregions. The basal pole maximum intensity is high, ranging from 25 to 97 multiples of a random distribution (mrd), indicating a strong basal texture. The basal pole peak near the axis center of the CFP rod is oriented parallel to the ED direction. As the distance from the axis center increases, the angle between the basal pole peak and ED also increases, resulting in a dome-shaped basal plane with a gradient [0002] direction in the global rod. The gradient basal texture of the CFP Mg rod is unique

compared to other processing methods such as hot extrusion and ECAP, and requires further investigation.

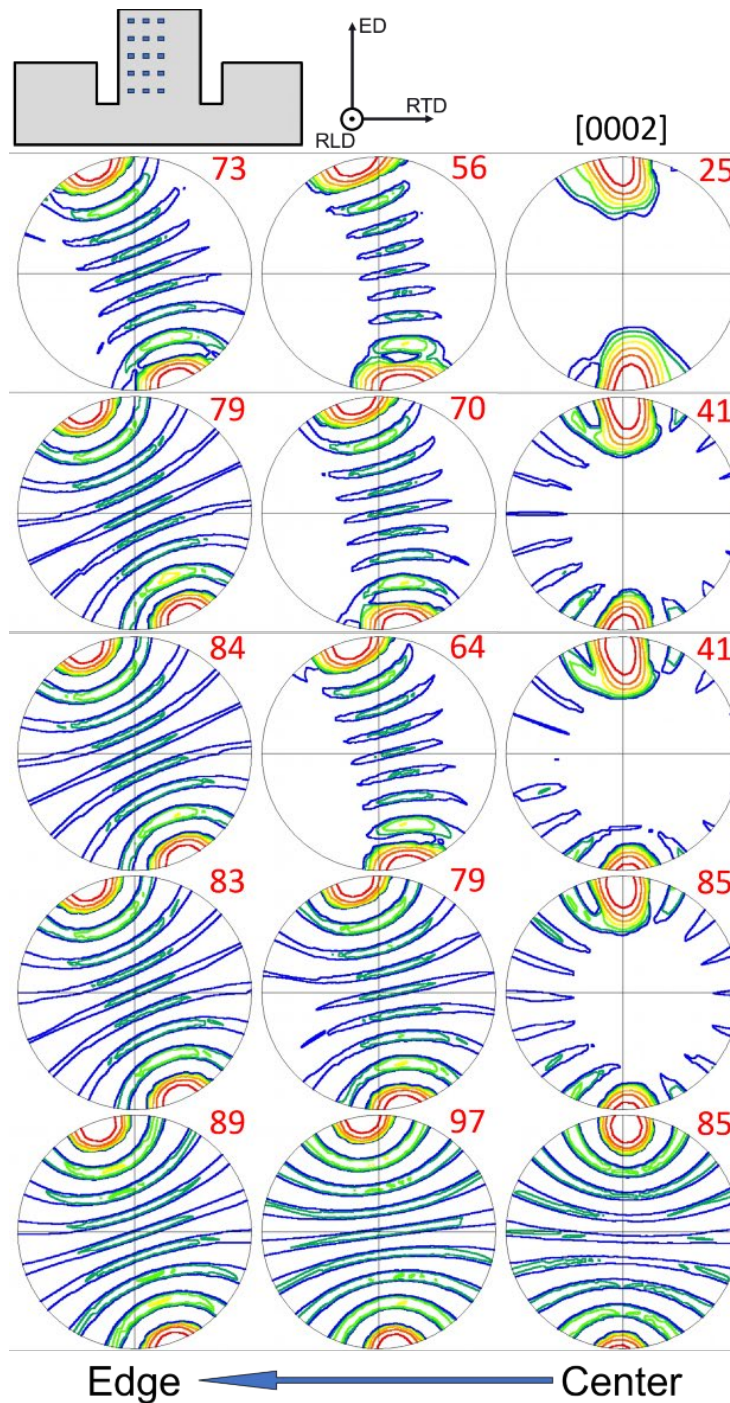


Fig. 3 [0002] pole figures (PF) with texture intensity of ZX10 obtained by CFP with rotation speed of 1800 rpm and plunge speed of 1 mm/s corresponded to the position marked by blue rectangle.

Mechanical Properties

Fig. 4 compares the compression properties of as-cast ZX10 and CFP ZX10 alloys obtained with rotation speeds of 1800 rpm and a plunge speed of 1 mm/s. The compressive yield strength of the

as-cast ZX10 alloy is significantly improved by CFP, increasing from approximately 50 MPa to about 200 MPa, an increase of over 300%. Similarly, the ultimate compressive strength is improved from approximately 208 MPa to about 334 MPa, an increase of about 60%. However, the elongation decreases. The improved compressive properties after CFP are related to the effectively refined grains. The results indicate that CFP is highly competitive in achieving excellent mechanical properties, meeting the design criteria for biodegradable bone-fixation devices proposed by Erinc et al [14]. This reflects the high potential of CFP in processing biomedical Mg alloys. Compared to the CFP ZX00 alloy with lower Zn content as reported in [13], the CFP ZX10 alloy demonstrated higher compression yield strength, increasing from approximately 180 MPa to 200 MPa, as well as ultimate compression strength, rising from around 290 MPa to 334 MPa. This enhancement can likely be attributed to solid solution strengthening resulting from the higher Zn content.

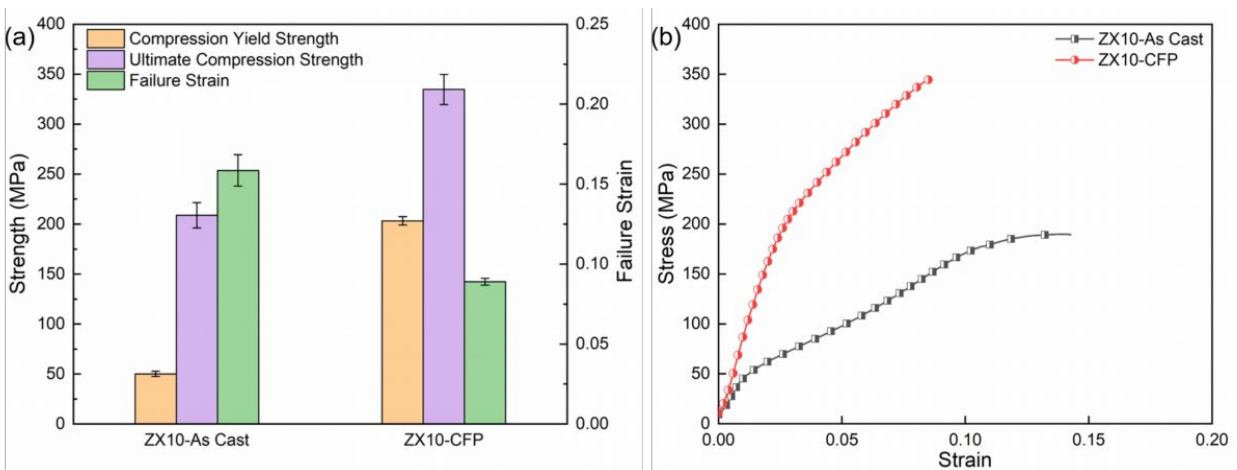


Fig. 4 (a) Compressive properties and (b) stress-strain curves of as-cast ZX10 alloy and CFP ZX10 alloy, produced at plunge speed of 1 mm/s and rotation speeds of 1800 rpm.

Discussion

Microstructure evolution ahead of stir zone

To analyze the evolution of microstructure during CFP, the “stop-action” technique was employed [15]. The CFP machine was stopped at a plunge depth of 2 mm via pressing the emergency button during processing, and the material was cooled using an ice-water mixture to “freeze” the microstructure and prevent subsequent static recrystallization and grain growth. The “frozen” transition zone from the thermo-mechanically affected zone (TMAZ) to the stir zone (SZ) was detected using EBSD, as shown in Fig. 5.

Firstly, Mg alloys were subjected to high compression stress from the shoulder, resulting in a large number of twins forming in the original large as-cast grains, as shown in Fig. 5. In this region, extensive twinning (T1 and T2) with the same $[11\bar{2}0]$ direction as the parent grain (P) was observed, and the high-angle twinning boundaries provided more nucleation sites for subsequent recrystallization [16]. For the parent grain in Fig. 5, the original basal plane was nearly perpendicular to the shear plane, i.e. the interface between SZ and TMAZ. As it approaches the SZ, which was subjected to more severe shear stress and higher temperature, pyramidal and prismatic slip become much easier to activate, and Mg exhibited higher plasticity [17]. Under the influence of shear stress, the grain lattice and basal plane rotated, leading to the formation of high grain boundary and continuous dynamic recrystallized (CDRXed) grains in the SZ with similar c-axis and strong basal fiber texture, whose basal plane is parallel to the shear plane.

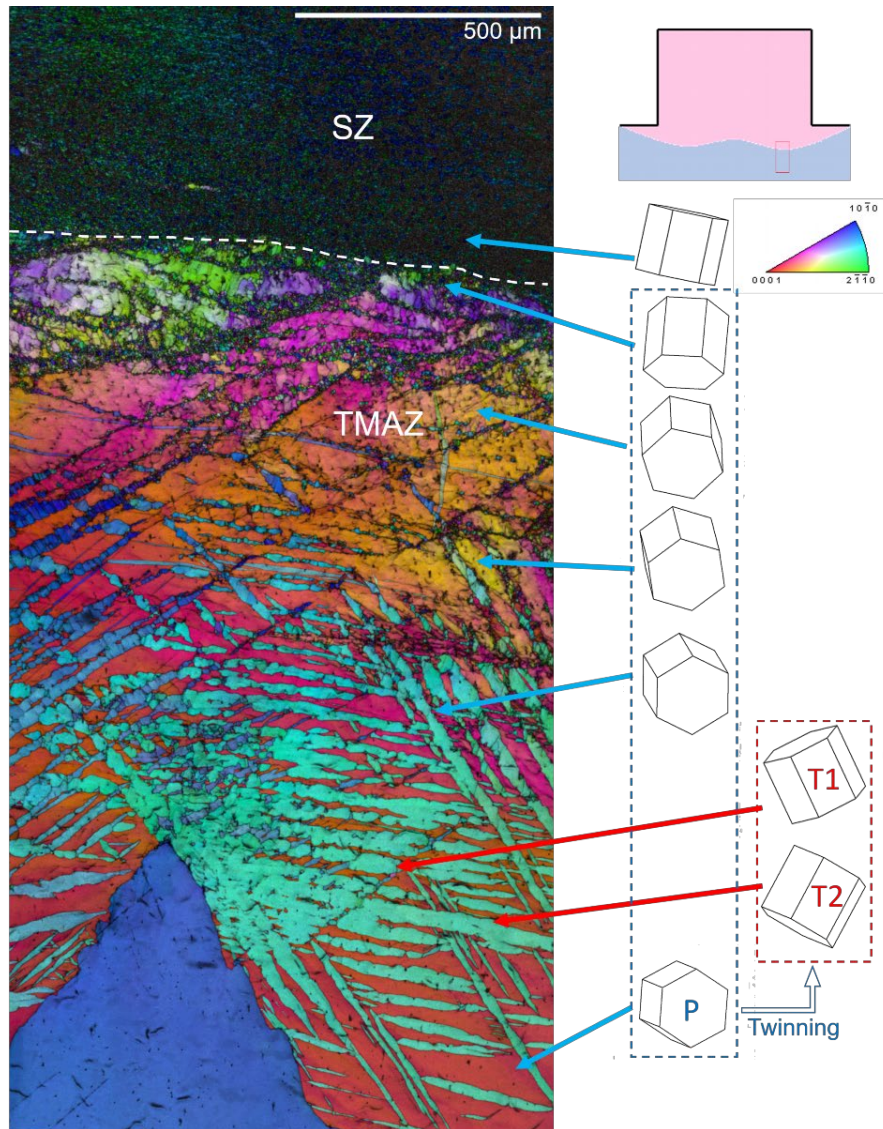


Fig. 5 Microstructure of transition zone between SZ and TMAZ obtained with “stop-action” technique.

Microstructure evolution in stir zone

Fig. 6 displays the GOS maps of different subregions in a CFP rod and the volume fraction of grains with different GOS ranges. From the bottom to the top of the CFP rod, the proportion of recrystallized grains with GOS lower than 2° increased. The bottom of SZ was subjected to severe shear strain, so the proportion of recrystallized grains is low. As the shoulder plunged down, the shear strain rate decreased, allowing more time for grains at upper part to recover and grow at high temperature. This results in an increase in the fraction of recrystallized grains as well as grain size from the bottom, see Fig. 2 and Fig. 5. From axis center to the edge of the CFP rod, the proportion of recrystallized grains decreases due to larger rotation radius and higher shear strain rate.

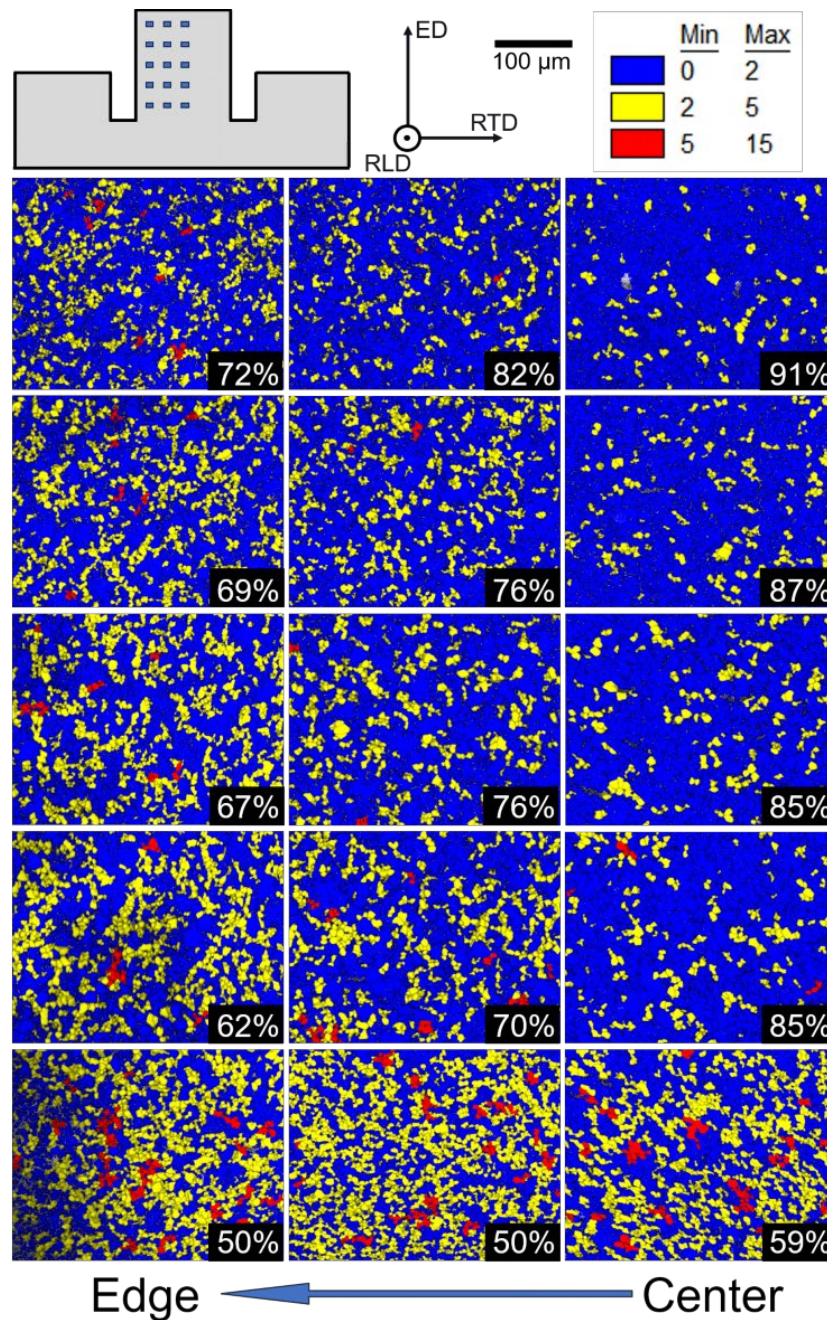


Fig. 6 GOS maps corresponding to different subregion in Fig. 2. Volume fraction of recrystallized grains ($GOS < 2^\circ$) is labeled at the lower right corner.

Summary

In this study, the novel constrained friction processing was utilized to refine the microstructure of the ZX10 alloy and improve its mechanical properties. The microstructure evolution was discussed. The following conclusions were obtained:

- (1) Defect-free ZX10 rods with grain size below $6 \mu\text{m}$ can be obtained using CFP with moderate heat input in a short time (3 s) from as-cast state with large grain size greater than 1 mm. The compression yield strength of ZX10 increased by more than 300% and the ultimate compression by 60% after CFP, which also higher than those of CFP ZX00.

(2) From the base materials to the TMAZ until SZ, microstructure experiences twinning and CDRX, resulting in strong basal fiber texture. In the processed rods, microstructure exhibits continuous development of DRX combined with grain recovery and growth.

Acknowledgements

Mr. Ting Chen thanks the China Scholarship Council for the award of fellowship and funding (No. 202006230137). The authors are grateful to Mr. Günter Meister and Mr. Gert Wiese from Helmholtz-Zentrum Hereon, Institute of Metallic Biomaterials, for the provision of the base materials used in this study and the guidance of the metallographic preparation. The technical support of Mr. Menno Peters and Ms. Camila Caroline de Castro, from Helmholtz-Zentrum Hereon, Institute of Materials Mechanics during this work is gratefully acknowledged.

References

- [1] A. Bahmani, M. Lotfpour, M. Taghizadeh, W.J. Kim, Corrosion behavior of severely plastically deformed Mg and Mg alloys, *J. Magnes. Alloy* 10(10) (2022) 2607-2648. <https://doi.org/10.1016/j.jma.2022.09.007>
- [2] Z. Savaedi, H. Mirzadeh, R.M. Aghdam, R. Mahmudi, Effect of grain size on the mechanical properties and bio-corrosion resistance of pure magnesium, *J. Mater. Res. Technol.* 19 (2022) 3100-3109. <https://doi.org/10.1016/j.jmrt.2022.06.048>
- [3] F.Y. Cao, Z.M. Shi, G.L. Song, M. Liu, M.S. Dargusch, A. Atrens, Influence of hot rolling on the corrosion behavior of several Mg-X alloys, *Corros. Sci.* 90 (2015) 176-191. <https://doi.org/10.1016/j.corsci.2014.10.012>
- [4] V. Bazhenov, A. Li, A. Komissarov, A. Koltygin, S. Tavalzhanskii, V. Bautin, O. Voropaeva, A. Mukhametshina, A. Tokar, Microstructure and mechanical and corrosion properties of hot-extruded Mg–Zn–Ca–(Mn) biodegradable alloys, *J. Magnes. Alloy* 9(4) (2021) 1428-1442. <https://doi.org/10.1016/j.jma.2020.11.008>
- [5] E. Mostaed, M. Vedani, M. Hashempour, M. Bestetti, Influence of ECAP process on mechanical and corrosion properties of pure Mg and ZK60 magnesium alloy for biodegradable stent applications, *Biomater* 4(1) (2014) e28283. <https://doi.org/10.4161/biom.28283>
- [6] C. Zhang, S. Zhu, L. Wang, R. Guo, G. Yue, S. Guan, Microstructures and degradation mechanism in simulated body fluid of biomedical Mg–Zn–Ca alloy processed by high pressure torsion, *Mater. Des.* 96 (2016) 54-62. <https://doi.org/10.1016/j.matdes.2016.01.072>
- [7] M. Vaughan, A. Karayan, A. Srivastava, B. Mansoor, J. Seitz, R. Eifler, I. Karaman, H. Castaneda, H. Maier, The effects of severe plastic deformation on the mechanical and corrosion characteristics of a bioresorbable Mg-ZKQX6000 alloy, *Mater. Sci. Eng. C* 115 (2020) 111130. <https://doi.org/10.1016/j.msec.2020.111130>
- [8] X. Zhang, Z. Wang, G. Yuan, Y. Xue, Improvement of mechanical properties and corrosion resistance of biodegradable Mg–Nd–Zn–Zr alloys by double extrusion, *Mater. Sci. Eng. B* 177(13) (2012) 1113-1119. <https://doi.org/10.1016/j.mseb.2012.05.020>
- [9] Z.J. Yu, C. Xu, J. Meng, X.H. Zhang, S. Kamado, Effects of pre-annealing on microstructure and mechanical properties of as-extruded Mg-Gd-Y-Zn-Zr alloy, *J. Alloys Compd.* 729 (2017) 627-637. <https://doi.org/10.1016/j.jallcom.2017.09.214>
- [10] S. Prithvirajan, S. Narendranath, V. Desai, Analysing the combined effect of crystallographic orientation and grain refinement on mechanical properties and corrosion behaviour of ECAPed ZE41 Mg alloy, *J. Magnes. Alloy* 8(4) (2020) 1128-1143. <https://doi.org/10.1016/j.jma.2020.08.015>

- [11] C. Wang, A. Ma, J. Sun, H. Liu, H. Huang, Z. Yang, J. Jiang, Effect of ECAP process on as-cast and as-homogenized Mg-Al-Ca-Mn alloys with different Mg₂Ca morphologies, *J. Alloys Compd.* 793 (2019) 259-270. <https://doi.org/10.1016/j.jallcom.2019.04.202>
- [12] C.C. de Castro, J. Shen, J.F. dos Santos, B. Klusemann, Microstructural development of as-cast AM50 during Constrained Friction Processing: Grain refinement and influence of process parameters, *J. Mater. Process. Technol.* 318 (2023) 118018. <https://doi.org/10.1016/j.jmatprotec.2023.118018>
- [13] T. Chen, B. Fu, U.F. Suhuddin, B. Wiese, Y. Huang, M. Wang, J.F. dos Santos, J.P. Bergmann, B. Klusemann. Application of novel constrained friction processing method to produce fine grained biomedical Mg-Zn-Ca alloy, *J. Magnes. Alloy.* <https://doi.org/10.1016/j.jma.2023.10.007>
- [14] M. Erinc, W. Sillekens, R. Mannens, R. Werkhoven, Applicability of existing magnesium alloys as biomedical implant materials, in: E.A. Nyberg, S.R. Agnew, N.R. Neelameggham, M.Q. Pekguleryuz (Eds.), *Magnesium Technology*. San Francisco, Minerals, Metals and Materials Society, Warrendale, PA, 2009, pp. 209-214.
- [15] P. Prangnell, C. Heason, Grain structure formation during friction stir welding observed by the ‘stop action technique’, *Acta Mater.* 53(11) (2005) 3179-3192. <https://doi.org/10.1016/j.actamat.2005.03.044>
- [16] S. Lu, D. Wu, R. Chen, The effect of twinning on dynamic recrystallization behavior of Mg-Gd-Y alloy during hot compression, *J. Alloys Compd.* 803 (2019) 277-290. <https://doi.org/10.1016/j.jallcom.2019.06.279>
- [17] S. Sandlöbes, M. Friák, J. Neugebauer, D. Raabe, Basal and non-basal dislocation slip in Mg–Y, *Mater. Sci. Eng. A* 576 (2013) 61-68. <https://doi.org/10.1016/j.msea.2013.03.006>